Percutaneous Absorption of Biologically-Active Interferon-gamma in a Human Skin Graft-Nude Mouse Model

Sarah M. Short,[1,4] Brian D. Paasch,[2] Jason H. Turner,[2] Norman Weiner,[3] Ann L. Daugherty,[1] and Randall J. Mrsny[5]

Received January 31, 1996; accepted April 7, 1996

Purpose. Topical delivery has been suggested to reduce systemic side effects while targeting cytokines for the treatment of certain skin conditions. Liposomes have been proposed as an enhancing agent for such a delivery. We have tested the potential of liposomes to augment the uptake of biologically active recombinant human interferon-gamma (rhIFN-γ) into human skin lacking adnexa in an in vivo model.

Methods. Stable grafts of human skin on nude mice were used to test aqueous formulations of rhIFN-γ containing or lacking liposomes composed of phosphatidylcholine and cholesterol. Transport of rhIFN-γ was assessed by monitoring the stimulated expression of intercellular adhesion molecule-1 (ICAM-1) by keratinocytes by light-level immunomicroscopy and ELISA.

Results. A single application of liposomal rhIFN-γ increased ICAM-1 levels in the epidermal basal and suprabasal cell layers of grafts. Continued application maintained this response. An aqueous formulation of rhIFN-γ or liposomes alone applied to grafts failed to induce an ICAM-1 response. Preliminary studies suggested that at least some of the lipids applied in the liposomal formulation also entered the epidermis.

Conclusions. Using a nude mouse-human skin graft model lacking adnexa, we have demonstrated that a liposomal formulation can augment the uptake of a biologically-active human cytokine, rhIFN-γ, into the epidermis of viable human skin. The therapeutic application of topical IFN-γ delivery remains to be evaluated.

KEY WORDS: human skin graft; nude mouse; rhIFN-γ; topical delivery; liposomes.

INTRODUCTION

The primary barrier to transdermal delivery of therapeutic agents is the non-viable, outermost layer of the epidermis known as the stratum corneum (SC) (1). Large, hydrophilic molecules, such as proteins, have very low or immeasurable transport rates across skin (2). Although our understanding of how this barrier functions is still incomplete, the unique morphology and lipid composition of the SC appear to function in limiting evaporative water loss as well as impeding the intrusion of materials and pathogens from the environment (3,4). Transport rates for small lipophilic therapeutics can be augmented significantly by co-administration of 'enhancing' molecules, such as aprotic solvents, pyrrolidones, Azone® and surfactants, through a disruption or alteration of the SC lipid structure (5). Most proteins, however, cannot tolerate the disruptive nature of these enhancing agents (6,7), and therefore do not benefit from such co-formulation approaches. Without a chemically-compatible permeation enhancer, protein therapeutics have not been widely investigated for topical applications.

Liposomal formulations have been suggested to promote intradermal drug penetration (8) and recently this approach has been used to increase the penetration of radio-labeled IFN-γ into hamster, hairless mouse and human skin *in vitro* (9) and interferon-α (IFN-α) *in vivo* (10). One concern related to the potential application of liposomes to enhance the topical delivery of IFN-γ is the uncertainty of the biological activity of this cytokine following formulation with lipids and entry into the skin. Previously, we addressed some aspects of this question by monitoring the transport of biologically active rhIFN-γ across human skin *in vitro* (11). Presently, we have examined the potential of liposomes to facilitate the transport of biologically active rhIFN-γ across human skin lacking adnexa *in vivo* using a grafted immunodeficient (nude) mouse model. The induction of ICAM-1 expression by keratinocytes (KCs) following stimulation by IFN-γ (12) was used as a surrogate marker for the transport of biologically active rhIFN-γ *in vivo*. ICAM-1 induction was followed qualitatively using light-level immunomicroscopy and semi-quantitatively by ELISA. Our results provide support for liposomes as a useful delivery system for the topical application of rhIFN-γ and establish the use of this model to evaluate the transport of a biologically-active cytokine in a qualitative and semi-quantitative fashion.

MATERIALS AND METHODS

In Vitro Studies

Time course studies of biological response (0–72 h) and assessment of liposomal rhIFN-γ formulation potency (relative to aqueous rhIFN-γ formulations) were evaluated histologically by monitoring ICAM-1 induction (11) in normal human KCs obtained from Clonetics (San Diego, CA). KCs were maintained in low-Ca^{2+}, serum-free medium supplemented with bovine pituitary extract and used between passage number 2 and 4 as sub-confluent monolayers on Lab-Tek Chamber slides (Nunc; Naperville, IL).

Skin Graft Model

The grafting model used was a modification of previously published methods (13,14). Post-mortem split-thickness skin preparations (abdominal, back or thigh) were from male donors with no known dermatopathy (Intl. Inst. Adv. Med.; Exton, PA). Dermatomed skin (~0.35 mm thickness) was immediately placed in ice cold Minimal Essential Media (Sigma, St. Louis,

[1] Pharmaceutical Research and Development, Genentech Inc., 460 Pt. San Bruno Blvd., South San Francisco, California 94080-4990.
[2] BioAnalytical Methods Development, Genentech Inc., South San Francisco, California 94080-4990.
[3] College of Pharmacy, University of Michigan, Ann Arbor, Michigan 48109-1065.
[4] Department Pharmacology, University of North Carolina, Chapel Hill, North Carolina 27599.
[5] To whom correspondence should be addressed.

ABBREVIATIONS: rhIFN-γ, recombinant human interferon-gamma; SC, stratum corneum; KCs, keratinocytes; ICAM-1, intercellular adhesion molecule-1; PBS, phosphate-buffered saline; RT, room temperature.

0724-8741/96/0700-1020$09.50/0

MO), shipped overnight on wet ice and grafted within 72 h of harvest onto both dorsolateral surfaces of four- to six-week old athymic (BALB/c) female nude mice (Charles River Labs; Raleigh, NC). Following the grafting surgery, all subsequent animal handling was performed in a laminar-flow hood using sterile procedures. Animals were used in transport experiments 24–31 days post surgery. All animal protocols adhered to the "Principles of Laboratory Animal Care" (NIH publication #85-23, revised 1985).

Formulations

Aqueous rhIFN-γ from Genentech, Inc. (South San Francisco, CA) was supplied at 9 mg/ml in a 10 mM succinate (pH 5.0) solution containing 0.01% Tween 20. Liposomes, prepared by lipid film rehydration and capillary dialysis as described previously (11), contained a final 10:1 ratio of cholesterol (Sigma; St. Louis, MO) to egg phosphatidylcholine (Avanti Polar Lipids; Birmingham, AL) with 0.1% α-tocopherol (Sigma; St. Louis, MO). The resulting homogeneous liposomes of ~100 nm diameter (11) were concentrated by ultra-filtration (Amicon Division, W.R. Grace & Co.; Danvers, MA) to 25 mg/ml, sterile-filtered through 0.45 μm Millex®-HV filters (Millipore; Bedford, MA) and stored in the dark at 4°C under N_2 until use. Physical mixtures of liposomes and rhIFN-γ had final concentrations of 0.512 mg/ml protein and 20 mg/ml lipid. Liposomes were used within two weeks of preparation and physical mixtures of rhIFN-γ with liposomes were prepared on the day of use.

Treatment Regimes and Tissue Collection

Stable skin grafts were treated with 100 μl volumes of either liposomal rhIFN-γ, aqueous (buffer) rhIFN-γ, buffer or liposomes alone applied daily for a period of 1 to 7 days. As a positive control, either aqueous or liposomal rhIFN-γ formulations were applied to tape-stripped (Scotch Magic tape 810, 3M Commercial Office Supply Division; St. Paul, MN) grafts. Animals were euthanized by cervical dislocation 1 to 14 d after completion of a dosing regimen. Grafts were immediately excised and cut in half. One-half was snap-frozen (isopentane at −65°C) in OCT embedding compound (Miles Labs; Elkhart, IN) and sectioned vertically (5 μm thick) using a cryostat microtome. Sections were placed on microscope slides coated with VectaBond (Vector Labs; Burlingame, CA), air-dried overnight at room temperature (RT) and stored at −70°C. The other half of each sample was snap-frozen (isopentane at −65°C) and stored at −70°C for subsequent analysis by ELISA.

Microscopic Studies

Tissue sections on microscope slides were fixed in methanol for 5 min at 25°C, washed, blocked in 0.5% casein (Sigma) in PBS for 15 min at RT and then in 20% normal goat serum (NGS, Vector Laboratories) in PBS (NGS-PBS) for 30 min at RT (15). For immunofluorescence, sections were incubated overnight at 4°C with FITC-labeled-anti-ICAM-1 (AMAC, Inc., Westbrook, ME) at a 1:50 dilution in NGS-PBS, washed exhaustively with PBS, rinsed with dH_2O and mounted with 90% glycerol, 0.1% *p*-phenylenediamine (Sigma) in 100 mM Tris·HCl (pH 8.5). For immunohistochemistry, casein-blocked sections were incubated for 1 h at 25°C with an anti-human ICAM-1 (CD54) mouse monoclonal antibody from Becton-Dickinson (San Jose, CA) at 2 μg/ml in PBS containing 1% bovine serum albumin (BSA-PBS). After washing in PBS-BSA, sections were labeled with a secondary antibody conjugated to alkaline phosphatase, washed exhaustively with BSA-PBS and exposed to Vector® Red alkaline phosphatase substrate (Vector Labs; Burlingame, CA) using the protocol supplied by the company. Labeled tissues were counter-stained with hematoxylin. Labeling controls for both immunofluorescence and immunohistochemistry were obtained by incubation of sections either in the absence of primary antibody or with an irrelevant primary antibody. Photographic images were obtained using a Leitz Aristoplan fluorescence microscope equipped with a fluorescein window and a Leitz Vario Orthomat 2 microscope camera.

Lipids were visualized using Nile Red (9-diethylamino-5-H-benzo[a]phenoxazine; Sigma) prepared as a 150 μg/ml solution in acetone. After diluting to 0.45 μg/ml in 75% glycerol, the dye was applied directly to skin sections which had been cut from OCT blocks, air dried, and rinsed with dH_2O (to remove OCT). Samples were viewed (excitation at 340–380 nm) immediately after dye application and photographed.

Enzyme-Linked Immunosorbent Assay (ELISA)

Frozen skin samples were weighed (typically 40–70 mg of tissue) and homogenized in 0.5 ml of a lysis buffer containing 150 mM NaCl, 10 mM Na_2EDTA, 50 mM Tris·HCl (pH 7.4), 1 mM 4-(2-Aminoethyl)-benzenesulfonyl fluoride (ICN Biomedical), 50 μM leupeptin (Boehringer Mannheim), 0.1 mg/ml soybean trypsin inhibitor (Sigma) and 20 μg/ml aprotinin (Sigma) on ice with three 1 min homogenization cycles using a Brinkman Polytron fitted with a PTA 7K1 generator. Homogenates were microfuged in a Biofuge A at 12,000 rpm for 5 min and isolated supernatants were stored at −70°C prior to submission for ELISA. Samples subjected to 4 freeze-thaw cycles had complete ICAM-1 recovery.

Components from a Bender MedSystems kit for human ICAM-1 (Endogen Inc.; Boston, MA) were used essentially as described (16) to create an ELISA method. Precoated stripwells (kit components) were washed (PBS, 0.5% Tween 20, pH 7.2 ± 0.1) using a Bio-Tek plate washer (Model EL 403H; Winooski, VT). Standards (kit component) and samples (50 μl) were diluted 1:10 in sample diluent (kit component) and plated out in duplicate at 80 μ/well. (Blank lysis buffer generated no false signal in the assay. A minimum dilution of 1:10 with sample diluent was required to overcome matrix-related signal suppression.) Following incubation at RT for 60–70 min with agitation (Mini-Orbital Shaker, Bellco Glass, Inc.; Vineland, NJ), plates were washed extensively and a 1:100 dilution of horseradish peroxidase-conjugate in assay buffer (kit reagents) was plated out at 80 μl/well. Following a second incubation at RT for 60–70 min with agitation and washing, 400 μg/ml of *o*-phenylenediamine in PBS with 0.012% H_2O_2 was plated out at 80 μl/well. Color was developed in the dark for 15–30 min (to effect) at RT and stopped by the 80 μl/well addition of 4.5 N H_2SO_4. Absorbance at 492 nm compared to a reference absorbance at 405 nm (Model EAR 340 AT, SLT Laboratory Instruments; Research Triangle Park, NC) was used for quantitation. A standard curve was generated using a nonlinear, four-parameter logistic regression analysis (17). The minimum detectable concentration was determined to be 1.56 ng/ml

ICAM-1. Precision profiles (18) estimated an intra-assay CV of 10% or less and an acceptable standard reporting range of 3.13–100 ng/ml ICAM-1.

Statistics

Comparisons were made with analysis of variance (ANOVA), using Fisher's protected least significance difference (PLSD) as the test statistic.

RESULTS AND DISCUSSION

In Vivo Model

The nude mouse-human skin graft model and techniques used in this study are similar to those previously described to refine methods of reconstructive skin grafting (13, 19) and to study pathological conditions such as psoriasis (20), giant congenital nevomelanocytic nevi (14) and alopecia areata (21). This model has also been used in transdermal transport studies (22). In our studies, human thigh, back or abdominal skin was grafted bilaterally in the mid-dorsal region of BALB/c nude mice (Fig. 1A). Within 3 weeks of surgery, stable grafts of approximately 2.25 cm^2 were achieved with a success rate of approximately 90%. Grafts had a normal human epithelial morphology (Fig. 1B) except that there was an obvious absence of adnexa (hair follicles, sweat and sebaceous glands). A clear demarcation between the thicker human (7–12 cells in thickness) and the thinner mouse (2–3 cells in thickness) epidermis and the transition from the absence to the presence of adnexa was clearly visible at the edges of grafts (Fig. 1C). Epidermal adnexa and other dermal substructures, such as arrector pili muscles develop during fetal gestation (23) and are not generated from split-thickness skin grafts during wound healing (13). Therefore, the lack of adnexa in skin grafts is not surprising but is an important aspect of this model since the transport of macromolecules into skin has been proposed to occur through sweat glands and/or hair follicles (24).

Isolated grafts, sectioned and exposed to an anti-mouse IgG antibody conjugated to horseradish peroxidase, showed that while the dermis was significantly remodeled with mouse skin components, the epidermis retained its human phenotype (Fig. 1D), consistent with previous observations in this human-nude mouse graft model (25). In light of this remodeling, it is important to note that there is no significant cross-reaction between mouse and human forms of IFN-γ and their respective receptors (26). Therefore, endogenous murine IFN-γ would not induce human ICAM-1 expression in KCs.

Keratinocyte ICAM-1 Induction *In Vitro*

In vitro cultures of KCs were used to verify time course and specificity of immunofluorescent (Fig. 2 A & B) and immunochemical (Fig. 2 C & D) methods to assess the up-regulation of ICAM-1 following rhIFN-γ exposure. Using these methods, significant ICAM-1 expression was observed after 12 h of exposure to rhIFN-γ and became even more prominent after 24 h, in agreement with a previously published time course of rhIFN-γ-induced ICAM-1 up-regulation in normal human skin (27). The labeling pattern observed for KCs *in vitro* was also identical to that reported previously (28). Physical mixtures of rhIFN-γ and liposomes induced significant ICAM-1 expression between 12 and 24 h, although this expression appeared, qualitatively, to be slightly less than that obtained for a similar liquid rhIFN-γ formulation (data not shown). Empty liposomes (lacking rhIFN-γ) did not induce ICAM-1 expression (Fig. 2 D).

Since the physical mixture of rhIFN-γ with liposomes produced a clear ICAM-1 induction as early as 12 h for all doses tested, it is likely that the presence of liposomes in these formulations did not prevent the administered rhIFN-γ from binding type II receptors on KCs. Further, these results demonstrate that the rhIFN-γ present in our liposome formulation retained biological activity. Previous studies have demonstrated the transport of biologically active rhIFN-γ into human skin *in vitro* from a physical mixture of this cytokine with preformed liposomes with a comparable time course of specific ICAM-1 induction (11).

ICAM-1 Induction in Grafts

Immunofluorescent localization of ICAM-1 in skin grafts treated with a physical mixture of rhIFN-γ and liposomes for 3 days *in vivo* demonstrated an uneven, but striking, labeling of the epidermis (Fig. 3). Grafts treated similarly with a liposomal formulation lacking rhIFN-γ or an aqueous rhIFN-γ formulation (data not shown) failed to show any significant epidermal labeling. The surrounding mouse skin did not show any epidermal ICAM-1 induction (data not shown). An immunohistochemical method was used to more clearly visualize the distribution of ICAM-1 induced by rhIFN-γ. Grafts treated for

Fig. 1. (*opposite, top*) Grafted human skin has normal epidermal morphology and extensive dermal remodeling. **(A)** Location and relative size of a human skin graft on a nude mouse. **(B)** Grafted skin excised and stained with hematoxylin and eosin (H&E). Basal (B), spinosal (S) and granular (G) cell layers of the epidermis and a fully-developed stratum corneum (SC) are depicted. **(C)** Mouse-human transition at the edge of a graft excised and stained with H&E. The transition between donor human (H) epidermis (lacking appendages) and host mouse (M) epidermis (containing appendages) is denoted with an arrowhead. **(D)** An untreated skin graft isolated 14 days after surgery, labeled with an anti-mouse IgG antibody conjugated to horseradish peroxidase and counter-stained with hematoxylin. Localization of the peroxidase product demonstrates extensive dermal (D) and minimal epidermal (E) remodeling. Magnification: **A,** ×1.5; **B,** ×200; **C,** ×100; **D,** ×400.

Fig. 2. (*opposite, middle*) Induction of ICAM-1 *in vitro*. An immunofluorescence method for fluorescein (**A** and **B**) and an immunohistochemical (**C** and **D**) protocol using Vector Red were used to demonstrate ICAM-1. Cultured human keratinocytes were exposed to either aqueous **(A)** or liposomal **(C)** formulations of rhIFN-γor similarly to aqueous **(B)** or liposomal **(D)** formulations lacking rhIFN-γ and assessed for the induction of ICAM-1 expression. Magnification: **A–D** ×630.

Fig. 3. (*opposite, bottom*) ICAM-1 expression is up-regulated by rhIFN-γ *in vivo*. **(A)** Immunofluorescence demonstrated the specific labeling of the epidermis (E) with very little labeling of the dermis (D) after 3 days of treatment with a liposomal formulation of rhIFN-γ and harvested on day 4. **(B)** A control skin graft treated for 3 days with a liposomal formulation lacking rhIFN-γ. (Magnification: **A & B** ×100.)

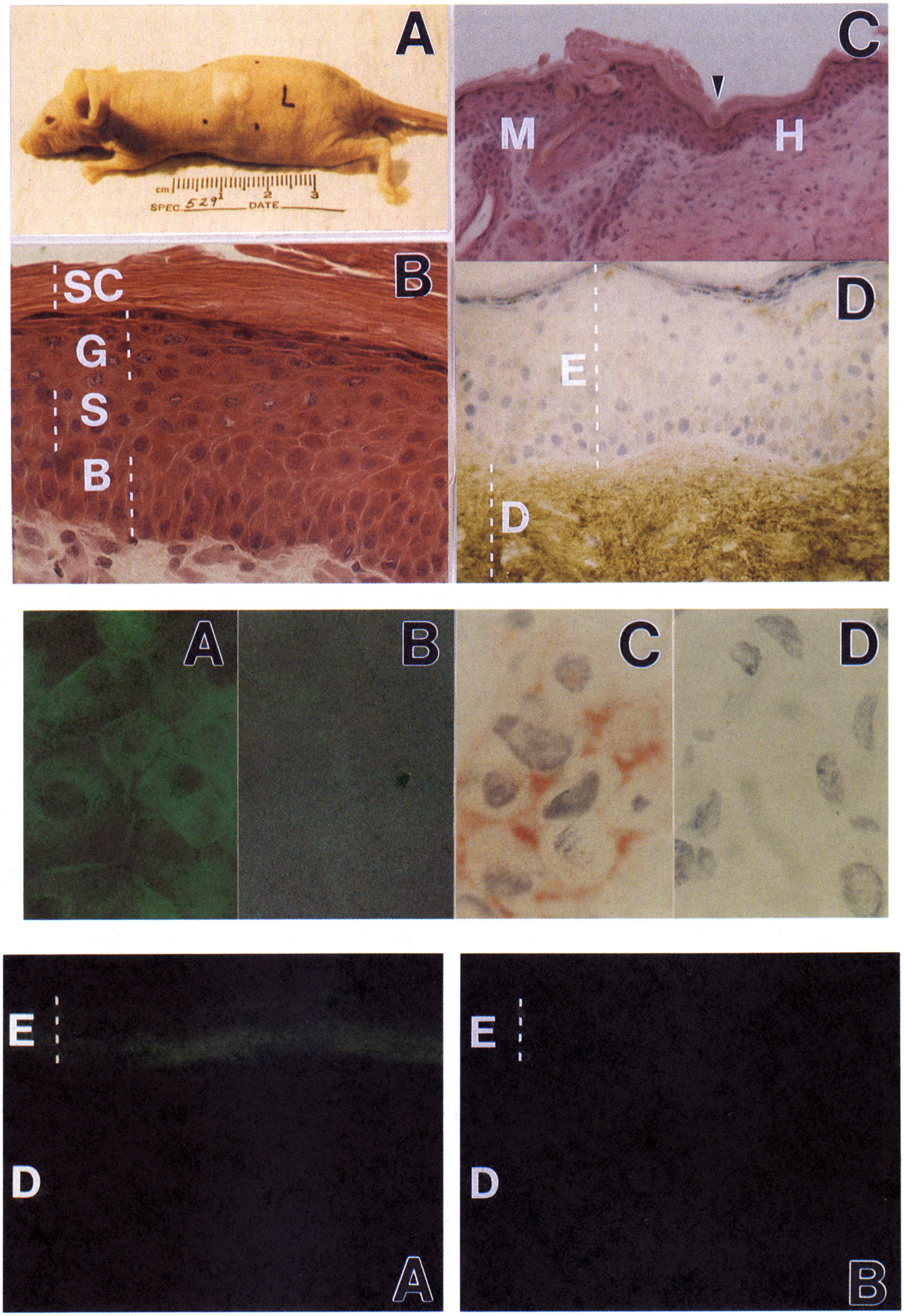
A
L
cm
SPEC. 529
DATE
B
SC
G
S
B
C
M
H
D
E
D
A
B
C
D
E
D
A
E
D
B

1 day with a liposomal formulation of rhIFN-γ demonstrated a low level of ICAM-1 induction limited to the basal and suprabasal cell layers (Fig. 4). The uneven induction of ICAM-1 observed microscopically may have been due to local regions of enhanced rhIFN-γ uptake or where the biological actions of rhIFN-γ were somehow augmented or might reflect variations in dermal ICAM-1 labeling from a minor and variable amount of constitutive ICAM-1 expression by dermal microvascular endothelial cells (29). Our results with liposomal formulations of rhIFN-γ applied to these grafts of human epidermis was similar to those described previously for ICAM-1 induction (27) and consistent with the distribution of IFN-γ receptors in human skin (30).

These microscopic studies provided only a qualitative demonstration of ICAM-1 induction. Since both soluble and membrane-associated forms of ICAM-1 can be induced by rhIFN-γ exposure, it is possible that at least some of the soluble ICAM-1 was washed away during the staining protocol employed and thus not detected. Therefore, a more quantitative method was required to assess relative levels of ICAM-1 induction. The ELISA used in our studies (Table 1) did not detect murine ICAM-1 and was considered robust enough to detect most if not all soluble ICAM-1 and possibly a large fraction of membrane-associated ICAM-1 present in homogenates prepared from skin grafts samples. ICAM-1 levels in untreated skin grafts were initially low and remained low during the duration of the study (21 days). In all treatment groups there was substantial variability in absolute ICAM-1 levels from animal to animal, and so paired active and placebo treatments were typically performed on opposing grafts from the same animal. This resulted in time- and treatment-matched controls for each comparison.

One application of liposomal rhIFN-γ increased ICAM-1 levels compared to placebo treated controls when assessed on the day following treatment (Table 1). Grafts treated similarly but evaluated 2 days following this single application had even higher levels of ICAM-1. Daily liposomal rhIFN-γ treatment for 3 days showed a significant response by day 4 (one day after the completion of treatments) which remained elevated on day 6 but diminished by day 8. During that same time period, a control group of grafts treated with an aqueous formulation, either containing or lacking rhIFN-γ, failed to demonstrate any differences in ICAM-1 levels (Table I). A number of other studies also failed to show a response of ICAM-1 induction following treatment with aqueous formulations of rhIFN-γ (data not shown). These results suggest that an aqueous formulation of rhIFN-γ failed to induce significant ICAM-1 levels and that induction of ICAM-1 by liposomal rhIFN-γ application becomes significant by 2 days of treatment and lasts for 3–4 days after treatments are stopped.

A longer duration treatment with liposomal rhIFN-γ was performed to assess whether a down-regulation of the response might occur after continuous treatment. Grafts treated for 7 days and evaluated one day after the completion of treatments (day 8) had elevated levels of ICAM-1 which were comparable to shorter (1 day or 3 days) duration treatments (Table I). Again, five days after the cessation of daily liposomal rhIFN-γ applications there was no longer an increased ICAM-1 level associated with grafts treated with active formulation compared to placebo controls. These results suggest that grafts treated with 7 daily applications had no apparent reduction in the responsiveness to liposomal rhIFN-γ induction of ICAM-1. By day 21 (14 days after the completion of daily treatments for 7 days) the ICAM-1 levels remained equivalent to controls.

To verify that the rhIFN-γ formulations being used were biologically-active in this *in vivo* system, grafts were tape-stripped to eliminate the barrier properties of the skin. Since disruption of the SC in this manner results in the release of cytokines capable of inducing ICAM-1 expression (31), the ICAM-1 levels in tape-stripped grafts receiving rhIFN-γ formulations were compared only to the elevated levels of tape-stripped grafts receiving placebo formulations (Table 1). On day 3, following 2 days of daily liposomal rhIFN-γ application and 1 day after cessation of treatment, ICAM-1 levels in tape-stripped grafts treated with active formula were roughly twice that of tape-stripped grafts receiving placebo lipid formulation. These results are consistent with previous studies showing the induction of ICAM-1 in tape-stripped skin and with our *in vitro* data that shows rhIFN-γ retains its biological activity following formulation with pre-formed liposomes (Fig. 2).

The ELISA results obtained in this study should be viewed as semi-quantitative at best, since several potential variables between skin samples could exist which could not be corrected. One variable relates to the approximate correction for skin surface area differences by a measure of sample weight. In this regard, a pilot study was performed which demonstrated that weight differences were approximately within 15% of surface area differences in the samples tested (data not shown). Further, we do not know the relative binding efficiencies of the soluble and membrane-associated forms of ICAM-1 in our ELISA. Although our homogenization protocol was designed to collect both soluble and membrane-associated forms of ICAM-1, we cannot rule out that some samples might be artificially high or low compared to other samples because of a difference in the distribution of these two forms of ICAM-1. Finally, it is possible that other cytokines, both human and murine, could have had some impact on human ICAM-1 induction beside rhIFN-γ in these skin samples.

Fate of Formulation Lipids

Previous *in vitro* studies have demonstrated the transport of biologically-active rhIFN-γ across human skin could be enhanced by the presence of liposomes (11). The results described in those studies were consistent with an augmented hydration state of the SC, and possibly increased water transport, as one putative mechanism whereby liposomes could act as an enhancing agent as previously suggested (32). Whether or not added lipids act to hydrate the SC, their ability to augment rhIFN-γ transport suggests that at least some fraction of formulation lipids may penetrate into the epidermis. Nile Red, an uncharged phenoxazone dye which has been used as a fluorescent stain for intracellular lipids (33) and to visualize diffusion pathways in human skin *in vitro* (34) was used to assess the penetration of lipid components. The fluorescence of this dye is highly dependent on the polarity of its environment; in cholesterol it fluoresces yellow-gold, while in phosphatidylcholine it fluoresces red. Nile Red labeling changed from a dull orange-red fluorescence in skin samples prior to treatment with liposomal formulations (Fig. 5A) to a more intense yellow-orange in the epidermis following exposure to a liposomal formulation (Fig. 5B). These results suggest that at least some of the applied lipids entered into and/or transported across the epidermis. The

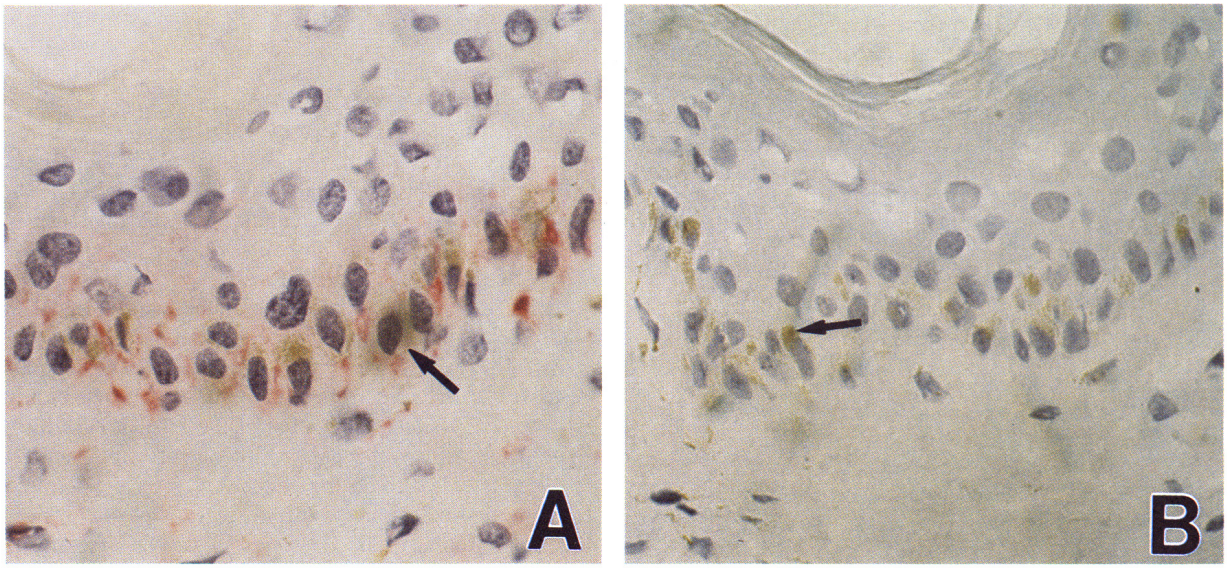

Fig. 4. Induction of ICAM-1 by rhIFN-γ *in vivo* is limited to the basal and suprabasal cells of the epidermis. **(A)** Graft treated with a liposomal formulation of rhIFN-γ*in vivo* for 1 day (harvested on day 2) demonstrated a low level of ICAM-1 induction observed using an Vector Red immunohistochemical protocol. **(B)** A negative control where the graft was treated with a liposomal formulation lacking rhIFN-γ. The brown color at the basal layer (arrows) demonstrates the distribution of melanin in these skin grafts stained with hematoxylin. Magnification: **A & B** ×320.

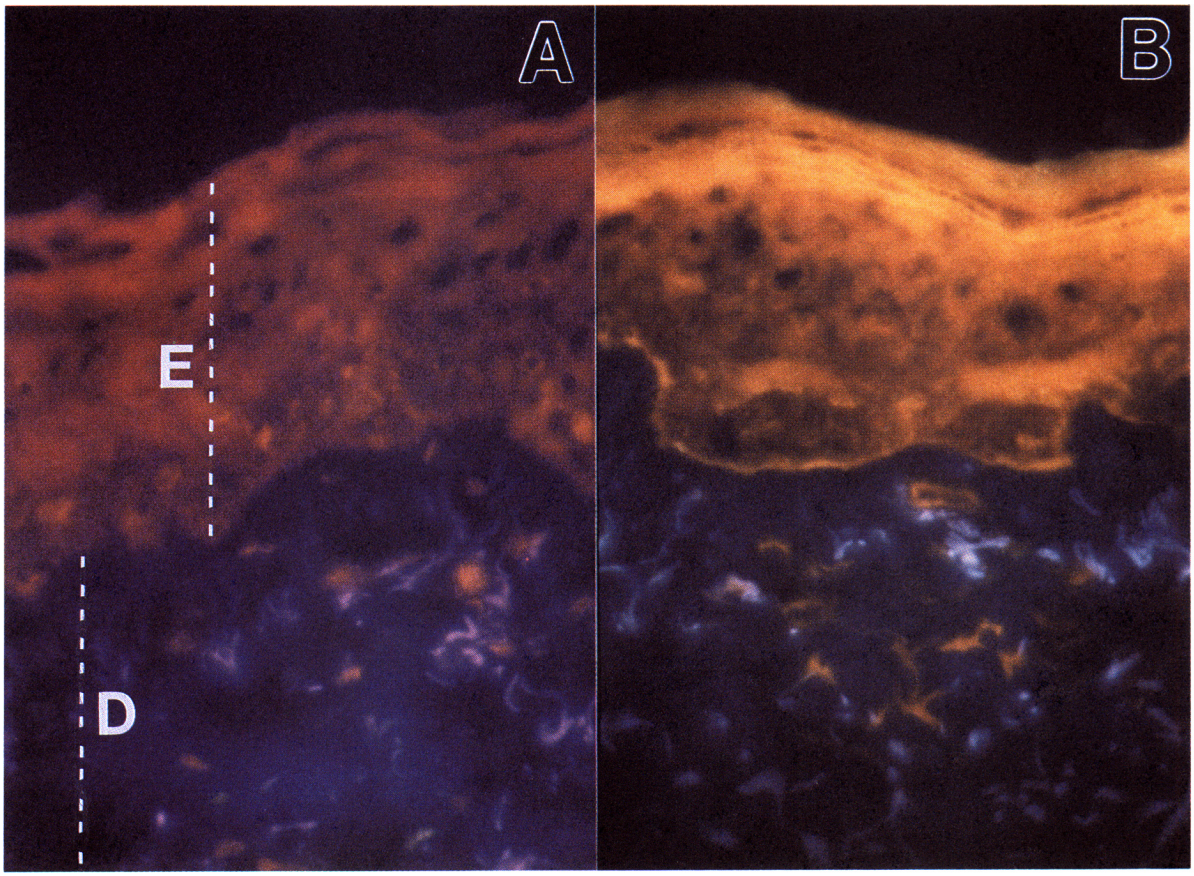

Fig. 5. Incorporation of lipids applied topically to human skin grafts. Skin grafts treated for 7 days with either placebo **(A)** aqueous or **(B)** liposomal formulations were exposed to Nile Red and viewed by fluorescence microscopy. Although comparable labeling was observed in the dermis (D), Nile Red fluorescence in the epidermis (E) suggested a modification of the lipid environment, presumably due to the incorporation of phosphatidylcholine and cholesterol from the liposomal formulation. Magnification: **A & B** ×320.

Table I. ICAM-1 Levels of Homogenized Human Skin Samples Determined by ELISA

Condition of Skin[a]	Applied Formulation[b]	Treatment Regime[c]	ICAM-1 (ng/mg tissue)[d] Active[e]	Placebo
Intact	None	0d/d1	—	0.6 ± 1.1 (n = 3)
Intact	None	0d/d21	—	0.6 ± 1.0 (n = 3)
Intact	Liposomal	1d/d2	1.7 ± 0.5‡ (n = 3)	0.6 ± 0.3 (n = 3)
Intact	Liposomal	1d/d3	3.7 ± 0.7† (n = 3)	1.4 ± 0.7 (n = 3)
Intact	Liposomal	3d/d4	3.4 ± 0.6† (n = 3)	1.8 ± 0.3 (n = 3)
Intact	Liposomal	3d/d6	3.1 ± 0.5† (n = 4)	1.1 ± 0.4 (n = 4)
Intact	Liposomal	3d/d8	2.3 ± 0.4 (n = 4)	2.0 ± 0.6 (n = 4)
Intact	Liposomal	3d/d10	2.0 ± 0.4 (n = 5)	1.6 ± 0.2 (n = 5)
Intact	Liposomal	7d/d8	3.0 ± 0.5† (n = 4)	1.1 ± 0.8 (n = 4)
Intact	Liposomal	7d/d12	2.6 ± 0.5 (n = 4)	2.5 ± 0.3 (n = 4)
Intact	Liposomal	7d/d21	1.5 ± 0.2 (n = 4)	1.4 ± 0.5 (n = 4)
Tape-stripped	Liposomal	2d/d3	7.1 ± 0.1‡ (n = 2)	4.1 ± 1.0 (n = 2)
Intact	Aqueous	3d/d4	1.17 (n = 1)	1.58 (n = 1)
Intact	Aqueous	3d/d6	1.28 (n = 1)	1.00 (n = 1)
Intact	Aqueous	3d/d8	2.04 (n = 1)	2.34 (n = 1)
Intact	Aqueous	3d/d10	0.87 (n = 1)	1.55 (n = 1)

[a]Intact skin refers to grafts considered to have an intact stratum corneum. Tape-stripping of skin was performed prior to each application of a formulation.

[b]Formulations were applied by massaging formulations onto the graft using a gloved finger. Animals typically had active formulation applied to a graft on one side and a placebo formulation applied on the contralateral graft.

[c]Grafts were dosed daily with 100 μl of a liposomal (20 mg/ml lipid) or aqueous (phosphate buffered saline) formulation for a set number of days and then grafts were harvested at a later day (e.g. 3d/d10 refers to grafts treated daily for 3 days and harvested 7 days following the last application).

[d]ICAM-1 values were obtained by ELISA and normalized by dividing by the weighed mass of the tissue homogenized to prepare each sample. Values are reported as mean ± SEM in μg ICAM-1/mg tissue mass measured prior to homogenization.

[e]Active formulations contained 0.512 mg/ml rhIFN-γ. Placebo formulations contained no added protein. Active versus placebo groups were compared by Fisher's PLSD and statistical differences are reported for the $p < 0.15$ level (‡) and the $p < 0.10$ level (†).

presence of rhIFN-γ did not appear to affect the distribution of the Nile Red staining (data not shown). Previous fluoromicrographic studies have suggested a penetration of intact liposomes into the SC of human skin (35). Our studies did not address the physical stability of liposomes following topical application.

CONCLUSIONS

We have previously investigated the transport of biologically active rhIFN-γ across human skin *in vitro* (11). In those studies, liposomes augmented cytokine transport in a manner which correlated with their ability to maintain a more hydrated state of the SC. Consistent with this, a recent report has shown that lipid (liposomal) formulations must remain hydrated to promote penetration across the SC (36). The present study has extended our previous observations to an *in vivo* model which employed human skin grafted onto nude mice. In all cases of ICAM-1 up-regulation, a pattern of labeling was observed consistent with a response primarily in the basal and suprabasal cell layers of the epidermis, the site of anticipated biological response. The topical application of a cytokine (e.g. rhIFN-γ) or similar protein with a putative therapeutic application may provide a practical route for a local delivery in the treatment of certain dermatopathies. Indeed, topical liposomal formulations of IFN-α have already been pursued as a treatment for vaginal warts (10) and more recently the topical delivery of a monoclonal antibody in the treatment of doxorubicin-induced alopecia has been described (37). Finally, local topical delivery of potent cytokines using a liposomal formulation may also provide new tools in the dissection of biological events associated with skin pathologies.

ACKNOWLEDGMENTS

The authors thank Drs. Rodney Pearlman and Tue Nguyen for their support and critical comments. Warren Young and David Finkle are acknowledged for their excellent technical assistance with the skin graft model and Deborah Gonzalez and Janet Dajio for their help with tissue analysis. We thank Ellen Gilkerson for generating the precision profiles for the ELISA. This work was supported in part by The National Institutes of Health, SBIR R43 AI30876.

REFERENCES

1. S. Monash. Location of a Superficial Barrier to Skin Penetration. *J. Invest. Dermatol.* **29**:367–376 (1957).
2. C. Cullander and R. H. Guy. Routes of Delivery: Case Studies. Transdermal Delivery of Peptides and Proteins. *Adv. Drug Delivery Reviews* **8**:291–329 (1992).
3. P. M. Elias and D. S. Friend. The Permeability Barrier in Mammalian Epidermis. *J. Cell Biol.* **65**:180–191 (1975).
4. R. O. Potts and M. L. Francoeur. The Influence of Stratum Corneum Morphology on Water Permeability. *J. Invest. Dermatol.* **96**:495–499 (1991).
5. A. C. Williams and B. W. Barry. Skin Absorption Enhancers. *Crit. Rev. Therap. Drug Carrier Syst.* **9**:305–355 (1992).
6. M. C. Manning, K. Patel, and R. T. Borchardt. Stability of Protein Pharmaceutics. *Pharm. Res.* **6**:903–918 (1989).
7. T.-C. Wang, J. and M. A. Hanson. Parenteral Formulations or Proteins and Peptides: Stability and Stabilizers. *J. Parenteral Sci. Technol.* **42**:S3–S26 (1988).
8. M. Mezei and V. Gulasekharam. Liposomes—A Selective Drug Delivery System for the Topical Route of Administration. *J. Pharm. Pharmacol.* **34**:473–272 (1982).
9. J. du Pleiss, K. Egbaria, C. Ramachandran, and N. Weiner. Topical delivery of liposomally encapsulated gamma-interferon. *Antiviral Research* **18**:259–265 (1992).
10. M. Weiner, N. Williams, G. Birch, C. Ramachandran, C. Shipmanjr, and G. Flynn. Topical Delivery of Liposomal Encapsulated Interferon Evaluated in a Cutaneous Herpes Guinea Pig Model. *Antimicrob. Agents Chemother.* **18**:212–224 (1989).

11. S. M. Short, W. Rubas, B. D. Paasch, and R. J. Mrsny. Transport of Biologically Active Interferon-gamma Across Human Skin *In Vitro*. *Pharm. Res.* **12**:1140–1145 (1995).
12. J. N. W. N. Barker, M. H. Allen, and D. M. MacDonald. The Effect of In Vivo Interferon-γ on the Distribution of LFA-1 and ICAM-1 in Normal Human Skin. *J. Invest. Dermatol.* **93**:439–442 (1989).
13. S. T. Boyce, T. J. Foreman, K. B. English, J. F. Stayner, M. L. Cooper, S. Sakabu, and J. F. Hansbrough. Skin Wound Closure in Athymic Mice with Cultured Human Cells, Biopolymers, and Growth Factors. *Surgery* **110**:866–876 (1991).
14. M. L. Cooper, R. L. Spielvogel, J. F. Hansbrough, S. T. Boyce, and D. H. Frank. Reconstitution of the Histologic Characteristics of a Giant Congenital Nevomelanocytic Nevus Employing the Athymic Mouse and a Cultures Skin Substitute. *J. Invest. Dermatol.* **97**:649–658 (1991).
15. D. E. Tacha and L. A. McKinney. Casein Reduces Nonspecific Background Staining in Immunolabeling Techniques. *J. Histotechnology* **15**:127–132 (1992).
16. R. Harning, E. Mainolfi, J.-C. Bystryn, M. Henn, V. J. Merluzzi, and R. Rothlein. Serum Levels of Circulating Intercellular Adhesion Molecule 1 in Human Malignant Melanoma. *Cancer Research* **51**:5003–5005 (1991).
17. D. Marquardt. An algorithm for least-squares estimation of nonlinear parameters. *J. Soc. Indust. Appl. Math.* **11**:431–441 (1963).
18. R. P. Ekins and P. R. Edwards. *The precision profile: its use in assay design, assessment, and quality control,* in *Immunoassays for Clinical Chemistry,* W. M. Hunter, and J. E. T. Corrie, Editors. 1983, Churchill Livingston: Edinburgh.
19. S. T. Boyce, E. E. Medrano, Z. Abdel-Malek, A. P. Supp, J. M. Dodick, J. J. Nordlund, and G. D. Warden. Pigmentation and Inhibition of Wound Contraction by Cultured Skin Substitutes with Adult Melanocytes After Transplantation to Athymic Mice. *J. Invest. Dermatol.* **100**:360–365 (1993).
20. G. Krueger, D. Manning, J. Malouf, and B. Ogden. Long-Term Maintenance of Psoriatic Human Skin on Congenitally Athymic (Nude) Mice. *J. Invest. Dermatol.* **64**:307–312 (1975).
21. A. Gilhar, A. Etzioni, B. Assy, and S. Eidelman. Response of Grafts from Patients with Alopecia Areata Transplanted onto Nude Mice, to Administration of Interferon-γ. *Clin. Immunol. Immunopath.* **66**:120–126 (1993).
22. D. B. Guzek, A. H. Kennedy, S. C. McNeill, E. Wakshull, and R. O. Potts. Transdermal drug transport and metabolism. I. Comparison of *in vitro* and *in vivo* results. *Pharm. Res.* **6**:33–39 (1989).
23. K. L. Moore. *The Developing Human.* 3rd ed. 1982, Philadelphia: W.B. Saunders Co. 432–436.
24. L. Lieb, C. Ramachandran, K. Egbaria, and N. Weiner. Topical Delivery Enhancement with Multilamellar Liposomes into Pilosebaceous Units: I. In Vitro Evaluation Using Fluorescent Techniques with the Hamster Ear Model. *J. Invest. Dermatol.* **99**:108–113 (1992).
25. M. Démarchez, D. J. Hartmann, M. Régnier, and D. Asselineau. Role of Fibroblasts in Dermal Vascularization and Remodeling of Reconstructed Human Skin after Transplantation onto the Nude Mouse. *Transplantation* **54**:317–326 (1992).
26. S. Pellegrini and C. Schindler. Early Events in Signalling by Interferons. *Trends in Biological Sciences* **18**:338–342 (1993).
27. Y. Teraki, N. Moriya, and T. Shiohara. Drug-Induced Expression of Intercellular Adhesion Molecule-1 on Lesional Keratinocytes in Fixed Drug Eruption. *Am. J. Pathol.* **145**:550–560 (1994).
28. M. Kashihara-Sawami and D. A. Norris. The State of Differentiation of Cultured Human Keratinocytes Determines the Level of Intercellular Adhesion Molecule-1 (ICAM-1) Expression Induced by γ Interferon. *J. Invest. Dermatol.* **98**:741–747 (1992).
29. L. A. Cornelius, J. T. Taylor, K. Degitz, L.-J. Li, T. J. Lawley, and S. W. Caughman. A 5′ Portion of the ICAM-1 Gene Confers Tissue-Specific Differential Expression Levels and Cytokine Responsiveness. *J. Invest. Dermatol.* **100**:753–758. (1993).
30. A. Scheynius, J. Fransson, C. Johansson, H. Hammar, B. Baker, L. Fry, and H. Valdimarsson. Expression of Interferon-Gamma Receptors in Normal and Psoriatic Skin. *J. Invest. Dermatol.* **98**:255–258 (1992).
31. L. C. Wood, S. M. Jackson, P. M. Elias, C. Grunfeld, and K. R. Feingold. Cutaneous Terrier Perturbation Stimulates Cytokine Production in the Epidermis of Mice. *J. Clin. Invest.* **90**:482–487 (1992).
32. K. Harada, T. Murakami, N. Yata, and S. Yamamoto. Role of Intercellular Lipids in Stratum Corneum in Percutaneous Permeation of Drugs. *J. Invest. Dermatol.* **99**:278–282 (1992).
33. D. L. Sackett and J. Wolff. Nile Red As a Polarity-Sensitive Fluorescent Probe of Hydrophobic Protein Surfaces. *Anal. Biochem.* **167**:228–234 (1987).
34. O. Simonetti, A. J. Hoogstraate, W. Bialik, J. A. Kempenaar, H. G. J. Schrijvers, H. E. Boddé, and M. Ponec. Visualization of Diffusion Pathways Across the Stratum Corneum of Native and In-Vitro-Reconstructed Epidermis by Confocal Laser Scanning Microscopy. *Arch. Dermatol. Res.* **287**:465–473 (1995).
35. J. Lasch, R. Laub, and W. Wohlrab. How Deep do Intact Liposomes Penetrate into Human Skin? *J. Controlled Rel.* **18**:55–58 (1991).
36. W. Gehring, M. Ghyczy, J. Gareiss, and M. Gloor. The Influence on Skin Penetration by Dithranol Formulated in Phospholipid Solutions and Phospholipid Liposomes. *Eur. J. Pharm. Biopharm.* **41**:140–142 (1995).
37. A. L. Balsari, D. Morelli, S. Ménard, U. Veronesi, and M. I. Colnaghi. Protection Against Doxorubicin-Induced Alopecia in Rats by Liposome-Entrapped Monoclonal Antibodies. *FASEB J.* **8**:226–230 (1994).